Decoration of Calcium Carbonate on Multi-Walled Carbon Nanotubes: An Efficient Removal of Crystal Violet from Aqueous Solution

Amira F. Sallam[(a)], Mohamed M. El-Halwany[(a)], Ashraf A. El-Bindary[(b)]*, Mahmoud H. Mahmoud[(a)]

Abstract— Multi-walled carbon nanotubes (MWCNTs-COOH) were decorated using calcium carbonate by a single stage chemical co-precipitation process for the preparation of calcium carbonate/multiwalled carbon nanotubes (CC/MWCNTs) for elimination of crystal violet (CV) from aqueous solution. CC/MWCNTs were categorized by field emission SEM, EDX, FT-IR, Raman spectroscopy and specific surface area. The results showed that MWCNTs-COOH was grafted with $CaCO_3$. The CC/MWCNTs had exceptional effecavy for elimination of CV, when CC/MWCNTs amount was 0.02 g/L. The CV exclusion rate reached 94.7% at CV primary load of $2x10^{-4}$ M and pH = 11 for contacting time of 60 min. The superficial zone and pore capacity of CC/MWCNTs were evluated by nitrogen adsorption/desorption experiments at 77 K and was found 55.134 m^2g^{-1} and 0.093 cm^3g^{-1}, correspondingly. The investigational equilibrium results were tested by the models of isotherm (Freundlich, Langmuir, Redlich–Peterson and Temkin) and the constants of isotherm were calculated. The adsorption balance showed that the isotherm of Langmuir suits the experimental results well. To examine the mode of action of adsorption process and the rate-monitoring phases, pseudo second order, pseudo first order, intra-molecular dispersion, and Elovich calculations was applied for inspection the investigational results. The adsorption kinetics was established according to pseudo-second-order kinetic model. In addition, the activation energy of the adsorption process was assessed and originates to be +19.50 kJ/mol demonstrating the kind of adsorption is chemisorption. Adsorption thermodynamics study recommended that the reactions of adsorption were spontaneous, exothermic and thermodynamically satisfactory. In addition, desorption conditions for CV and reusability of the adsorbent was estimated, which established the recyclability of the adsorbent.

Index Terms— Multiwalled carbon nanotubes, Crystal violet, Adsorption, Kinetics, Thermodynamics.

1 Introduction

Throughout the earlier 20 years, multiwalled carbon nanotubes (MWCNTs) have become a significant manufacturing substantial. Numerous tons are formed annually. Multiwalled carbon nanotubes, a novel inorganic purposeful nanomaterial with distinct properties, have concerned abundant consideration in current years [1]. There are numerous features, such as, minor circular extent, exceptional mechanical possessions, remaining electrical and thermal conductivity and great explicit superficial [2,3], so they are useful in numerous arenas such as, battery and materials engineering, carbon fiber, biological catalytic resources and conductor resources for energy storing expedient [4], and as nano adsorbents for the treatment of water also frequently develop study idea. In the other hand, $CaCO_3$, is a naturally inorganic materials with prodigious biocompatible properties, has been extensively applications in manufacturing, technology, medication, microcapsule production, and several extra bio-associated arenas [5]. The amalgamation of Ca with MWCNTs is actuality inspected to feat the astonishing mechanical possessions of MWCNTs to strengthen bio actively resources. The adding of $CaCO_3$ to MWCNTs is consequently predictable to advance the merged coat by substantial the carbon micro tubes, creating impenetrable bio actively layer, avoiding Al and V from escape off to blood flow. This mixture advances the deterioration fight and encourages a perfect inter-superficial connection amongst Ca and MWCNTs that could be eventually responsibly for greater steadiness and resistance. Crystal violet dye is commonly applied for staining in the fabric manufacturing, request in the production of dyes and production toners, it is employed as a biologically dye and its vigorous ingredients in Gram's color, veterinary medication, and it is likewise working by way of a bactericide and dermatologically mediator in people [6]. Furthermore, it is castoff as additives to fowl's feedstuff to prevent spread of mold, intestinal pests and mold [7]. The color is accountable for producing reasonable eye exasperation, initiating tender susceptibility to bright. It is extremely poisonous to mammalian compartments and, if fascinated in damaging quantities via the skin, it cans origin skin crossness and intestinal area annoyance. In dangerous belongings it might also principal to respirational and meat fiascoes, it is cancer-causing, and it takes categorized as an intractable particle meanwhile it is unwell digested by microorganisms. Because of the organizational difficulty of the dyed complexes and their solubilization in water, the fragmentation procedure is difficult. Several an-

(a) Mathematics and Engineering Physics Department, Faculty of Engineering, El-Mansoura University, El-Mansoura, Egypt.
(b) Chemistry Department, Faculty of Science, University of Damietta, Damietta 34517, Egypt
Corresponding author: E-mail: *abindary@yahoo.com*

other physical/chemical procedures, such as flocculation/coagulation and ultrasonic management, require been laboring, nevertheless greatest of these dealings are inadequate owing to great process budgets, and the necessity for dedicated apparatus [8]. Newly, amalgamated nanofibers fascinate courtesy in water and wastewater handling by reason of their exceptional assets such as trivial fiber width, higher characteristic proportion, bulky explicit superficial zone, great elasticity for chemical/physical superficial function, and physicochemical possessions [9]. Trendy our earlier effort [10–12], we have confirmed that, the applying of nano composite ingredients for the exclusion of heavy metals and deprivation of organic colorants [13,14]. Consequently, in this labor we envisioned to spread our former effort by means of the nanocomposite resources for the dilapidation of organic colorants like crystal violet (CV) via a nanocomposite substantial (CC/MWCNTs). Investigational constraints distressing the adsorption procedure such as preliminary adsorbate load, adsorbent amount, connection period, temperature and pH of the solution were considered. The investigational equipoise adsorption information was scrutinized by kinetic and isotherm models. Thermodynamics study of the adsorption process specified impulsive and exothermic environment of the procedure.

2. Materials and methods

2.1. Materials

Multiwalled carbon nano-tubes (with purity 96 wt %, width: 20–30 nm and distance: 21 μm) was purchased from Sigma-Aldrich. Dimethylformide (DMF), HNO_3 65%, H_2SO_4 98% and $CaCO_3$ remained brought by Merck House (Germany). Crystal violet (CV) with a purity of over 90%, bought from Sigma-Aldrich and recycled without further cleaning. A standard solution of CV whose attention was 1.0 $g.L^{-1}$ was castoff and can be dilute to the requisite attention with distilled water in the research. Altogether chemical components are analytical mark and were recycled as established.

2.2. Preparation of MWCNTs-COOH

The adjustment of MWCNTs with COOH group is prepared giving to Srinivasan et al. [8]. MWCNTs (0.5 g) were occupied in 80 mL combination of HNO_3/H_2SO_4 (1:3, v/v) for different times at 75 °C under constant sonication. After filtration, the solid of black color was gained, washed numerous times with purified water and finally dehydrated at 85 °C in vacuum desiccator over anhydrous $CaCl_2$. The resulting MWCNTs–COOH was used for additional adjustment.

2.3. Preparation of calcium carbonate/multiwalled carbon nanotubes

Calcium carbonate/multiwalled carbon nanotubes (CC/MWCNTs) were organized in the disorder that the form proportion of MWCNTs-COOH to $CaCO_3$ was 3:1 in 25 ml dimethylformamide. The reaction mixture was refluxed on an oil bath for 72 hrs. at 80 °C shadowed by ultrasonic action for 15 min. The product formed was filtrated, washed to neutral by distilled water and acetone. Finally, dehydrated at 85 °C, grinded, separated, and then MWCNTs functionalized by $CaCO_3$ were expanded. Elemental distribution of CC/MWCNTs by EDX analysis: C, 71.41; O, 18.94; Ca, 9.25.

2.4. Characterization

Automatic Analyzer CHNS Vario ELIII, Germany was used for C, H and N determination. The characteristic functional groups of CC/MWCNTs were determined by JASCO FT/IR-4100 spectrometer (Jasco, MD, Easton, USA) using KBr discs in the range ofwavenumber 400–3800 cm^{-1}. Raman spectrum of sample was approved backs-cattering geometry by the 1064 nm excitation wavelength by resources of a Bruker-Vertex-70 Infrared Spectrometer. The surface morphology of CC/MWCNTs was analyzed before and after the adsorption processes of crystal violet (CV) by (JEOL/JSM-6510 LV) scanning-electron-microscope (SEM) to perceive surface alteration. Energy dispersive X-ray spectroscopy (EDX) (Leo-1430VP microscope by effective voltage 5 kV) was secondhand for the elemental distribution of CC/MWCNTs analysis. Absorbance capacities of tasters with 1 cm quartz-cell were tested by UV-Visible spectrophotometer (Perkin-elmer-AA800 spectrophotometer Model-AAS) to determine the concentrations of CV left in the supernatant solutions. The N_2 isotherm of adsorption/desorption on CC/MWCNTs at 77 K was done with a Quantachrome-Touch-Win Tools version 1.11. The curves analysis was developed by Brunauer/Emmett/Teller (BET) technique (pp^o from 0.06 to 0.36) for exact area, micropores volume and area, t-plot method for outside area and Barrett/Joyner/Halenda (BJH) process for diameter resolve of mesopores. Maxturdy 30 (Wisd) and pH-meter (HANNA, model-211) instruments were secondhand for shaking and pH-adjustment, respectively.

2.5. Sorption studies

Batch adsorption experiments were conducted by an orbital shaker instrument at 250 rpm and 25 °C, using 50 mL conical flasks with 0.02 g of (CC/MWCNTs) and 25 mL of different concentrations of dye solution with accurate pH by HCl (0.1 M) and NaOH (0.1 M) solutions. The supernatant solution was separated by filtration at the end of the process. Then the concentrations of the residual dye in supernatant solutions were determined using UV–Vis spectrophotometer by assistance the absorbance at 590 nm of CV dye. Eq. (1) was used for the calculation of the percentage of dye removal (R).

$$R = 100\ (C_0 - C_t)/C_0 \quad (1)$$

wherever C_0 (mg/L) and C_t (mg/L) indicates the premier CV dye concentration and at any time t, respectively.

The adsorption isotherms were studied with dye solutions of different initial concentrations ($5x10^{-5}$ – $5x10^{-4}$ M) were disturbed with 0.02 mg of CC/MWCNTs until the adsorption equilibrium was reached at 25 °C. The concentrations of CV left in the supernatant solutions were determined to calculate the capacity of adsorption equilibrium, qe (mg dye by g adsorbent) by using Eq. (2):

$$Qe = V\ (C_0 - C_t)\ /W \quad (2)$$

wherever C_t (mg/L) is the equilibrium dye concentration, V (L) is the solution volume and W (g) is the CC/MWCNTs weight. Adsorption thermodynamic parameters were calculated by studying the adsorption isotherms at

other temperatures (20, 30, 35, 40 and 45 °C).

The techniques of kinetic experiments were performed at 25 °C in the condition of a certain concentration of CV dye ($2x10^{-4}$ M) and pH (11). After different time intervals (5–90 min) the concentrations of the CV dye left in supernatant solutions were measured by UV–Vis spectrophotometer. At time t the quantity of CV dye consumed per unit mass of the adsorbent, qt (mg/g) was calculated using Eq. (3):

$$Q_t = V(C_0 - C_t) / m \quad (3)$$

wherever C_0 (mg/L) represents the originel dye concentration, C_t (mg/L) the concentration of dye at any time t, V (L) the solution volume of CV and m, g is the weight of CC/MWCNTs adsorbent.

3. Results and Discussion

3.1. CC/MWCNTs Characterization

3.1.1. Brunauer-Emmett-Teller

Nitrogen adsorption/desorption isotherm strongminded at 77 K on the organized taster (CC/MWCNTs) is exemplified in Fig. 1. The explicit superficial zone is appraised by claim the BET calculation in its usual assortment of applicable value of 16.21 Å for the cross-section-area of nitrogen fragment. Capacity of entire hole, occupied at P/P^o = 0.948, and the opening magnitude spreading is assessed using BJH-technique. The isotherm of adsorption of the trial is categorized as kind (II) through H4-hysteresis circlet categorized by IUPAC that covering downhearted to $[P/P^o]$ = 0.39; this profound hysteresis circlet ascends beginning of collections (accumulation of elements which are insecurely intelligible) of plate-like arrangement generous growth to slit-shaped holes [15]. The superficial zone ABET = 55.15 m^2/g, the entire hole capacity = 0.094 cm^3/g and the middling opening radius = 33.78 Å which authorizes the meso-porosity of organized trial. Slight opening magnitude spreading discloses the sameness of the hole magnitude over the trial environment.

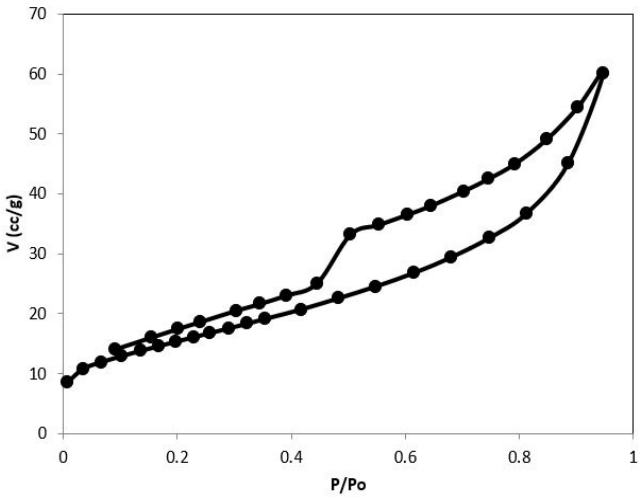

Fig. 1. BET isotherms of adsorption/desorption of CC/MWCNTs.

3.1.2. FT-IR Spectroscopy

FT-IR bands of underdone MWCNTs-COOH and CC/MWCNTs showed absorption band at 3420 cm^{-1} associated to the presence of O–H stretching vibrations of hydroxyl group. The stretching vibration of C=O carbonyl group of carboxylic acid was appeared at 1729 cm^{-1} [16]. Additionally, medium bands at 1558 and 1443 cm^{-1} assignable to $\nu_{asym}(COO^-)$ and $\nu_{sym}(COO^-)$ of carboxylate group, respectively [17]. This consequence obviously displayed incidence of -COOH groups on the superficial of MWCNTs-COOH. The irregular enlarging quivering posse of C–H bond seems at 2850 cm^{-1}. The characteristic posse 2350 cm^{-1} [17,18] are assigned to skeletal C=C aromatic vibrations of MWCNTs-COOH. In addition to the above bands, more bands appeared popular the spectrum of CC/MWCNTs. Bands at 1320, 848 and 720 cm^{-1} since were assigned to the trembling of CO_3^{2-} anion in inorganic carbonate, resemble to C–O antisymmetric extending trembling, out-plane and in-plane distortion trembling of CO_3^{2-} in dissimilar crystal arrangements, correspondingly, which earnings adapted carbon nanotubes had $CaCO_3$ [1]. The functional superficial of CC/MWCNTs with the carboxylate and carbonate groups ($-COO^-$ and CO_3^{2-}) is a main feature which is in authority for the cationic dye's preoccupation on to the industrialized adsorbent. As a result of the attendance of the ($-COO^-$ and CO_3^{2-}) it can straightforwardly liquify in the aqueous electrolyte and negative external charge, i.e. COO^- and CO_3^{2-} upsurges, which origins intensification in the electrostatic magnetism amongst the positively charged mineral violet fragments and negative superficial charge of CC/MWCNTs.

3.1.3. Raman spectroscopy

The qualitative information about the functionalization of CC/MWCNTs surfaces can be determined by raman spectroscopy technique which is sensitive to the carbon materials The Raman spectrum of CC/MWCNTs particles exhibits the so-called D- and G-bands at 1344 and 1568 cm^{-1}, respectively [19]. A defect in G-band is observed at 2688 cm^{-1} in the Raman spectrum. On careful examining the spectrum, one can notice a band centered at 1070 cm^{-1} that referred to the amorphous carbon in CC/MWCNTs layers. It is interesting to notice many peaks in the low frequency range (250-350 cm^{-1}) of the spectrum. The most observable one is located at about 288 cm^{-1} which normally exists in the Raman spectra of multi-walled carbon nanotubes. It is interesting to mention that the G-band creates beginning in-plane peripheral extending of the carbon bonds in MCNT, representing of a great notch of assembling and good-organized C based structures. However, the D band or the complaint crew habitually recounts to the attendance of the unstructured or complaint carbon in MWCNT. The strength relation of the D band to the G band is frequently applied as an operative extent for imperfection compactness or development of unwanted arrangements of carbon particles [20,21]. G band is the over manner from D band which is a binary character persuaded by complaint and imperfections.

3.1.4. EDX

Beginning the EDX investigation of the matching superficial, can be understood the border spectacle was unruffled of

CC/MWCNTs. EDX investigation of CC/MWCNTs: component (Wt, %): C 71.41; O 18.94; Ca 9.25, element (At %): C 80.62; O 16.05; Ca 3.13 and element (K-Ratio) C 0.4633; O 0.0222; Ca 0.0923.

3.1.5. SEM Analysis

Scanning-electron-microscopy (SEM) consumes a main instrument for describing the external morphology and important physical possessions of the adsorbent outward. This one is beneficial for decisive the element form, sponginess and suitable dimensions spreading of the adsorbent. Scanning-electron micrographs of (CC/MWCNTs) and with dye adsorbed are exposed in Fig. 2. Fig. 2 (a) shows granular materials of CaCO3 coating on MWCNTs and the raw (CC/MWCNTs) has significant facts of apertures wherever, nearby is a decent opportunity for colorants to remain imprisoned and adsorbed hooked on these apertures. The SEM image of (CC/MWCNTs) adsorbed through experienced colorant (CV) display identical illustrious dim acnes Fig. 2(b) which can be engaged as a mark for operative CV dye adsorption fragments in the craters and openings of this adsorbent [22].

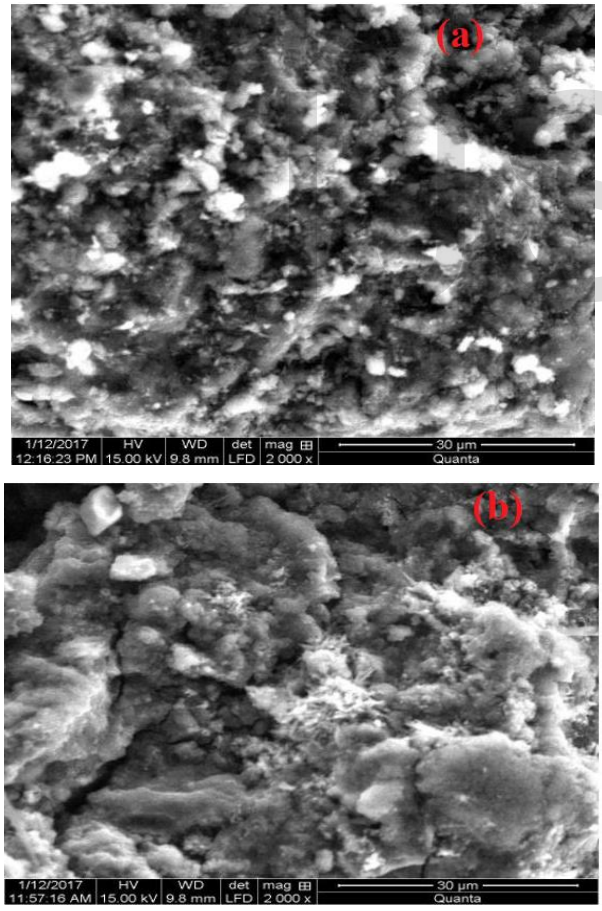

Fig. 2. SEM image of CC/MWCNTs: free (a) and after adsorption of CV dye (b).

3.2. Effect of initial solution pH

It is recognized that, the elimination of CV from aqueous media be contingent on the original medium pH then the outward charge of the adsorbent diverges with the alteration of pH magnitude. Furthermore, the medium pH similarly disturbs the grade of ionization of CV and concentration of the counter H^+ ions of the outward clusters. Accordingly, an optimal pH is imperative limitation throughout the dye adsorption development. Trendy, the outcome of medium pH on the adsorption of dye was considered in the pH assortment 3-12 through preliminary load of $1x10^{-4}$ of the colorant, 25 ^oC and 0.02 g adsorbent quantity. CC/MWCNTs have demonstrated toward an operative adsorbent for the exclusion of the colorant, which was realized through adsorption since an aqueous medium of pH 11 was, accomplished (Fig. 3). In alkaline solutions, a much larger amount of OH^- group and the surface of CC/MWCNTs have negative charge due to a much larger amount of deprotonated $–COO^-$ and CO_3^{2-} negative groups. Therefore, the electrostatic adsorption amongst the negative charge of the adsorbent superficial and cations of the dye molecule was increased. In lesser pH levels, extra protons (H^+) existed to protonate the negative groups on CC/MWCNTs to form positive charges, thereby enhancing the electrostatic repulsion amongst positively charged surface of CC/MWCNTs and positively charged dye cations [19].

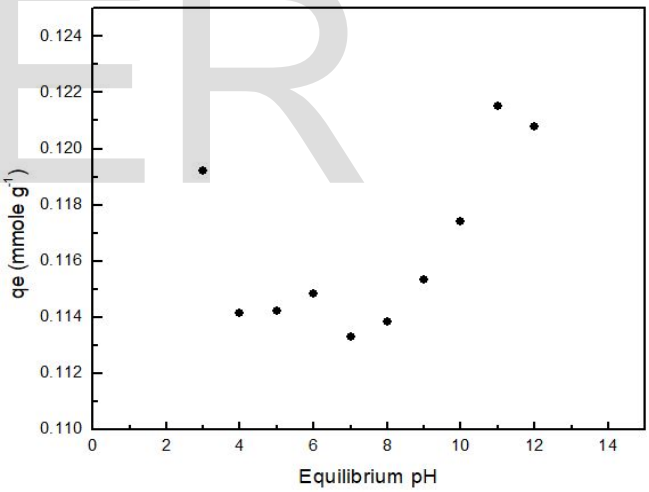

Fig. 3. pH effect on adsorption using the adsorbent: (T: 25 ^oC; C_0: 1 $x10^{-4}$ M).

3.3. Effect of dye concentrations

The subtraction of CV dye through adsorption arranged CC/MWCNTs was exposed to upsurge per period and achieved a supreme rate at nearby 70 min, and afterward, it continued virtually continuous. Happening altering the preliminary load of colorant medium beginning $5x10^{-5}$ to $5x10^{-4}$ M at 25 ^oC, pH 11 and 0.02 g adsorbent quantity the expanse of detached colorants was diminished. It was indistinct the exclusion of the colorant was reliant on the preliminary load of the colorant since the reduction in the preliminary colorant load augmented the quantity of the adsorbed dye. This is identical vibrant for the reason that, for a immovable adsorbent measure, the amount of energetic adsorption locations to

put up adsorbate ions remainders untouched nevertheless through growing adsorbate load, the adsorbate ions towards quartered upsurges and hereafter the proportion of adsorption enthusiasms downhearted.

3.4. Effect of adsorbent dosage

The commitment of CV colorant through variation in adsorbent prescription (0.02–0.1 g) at adsorbate loads of $5x10^{-4}$ M at 25.0 °C and pH 11 is offered (Fig. 4). Enluminant adsorption displays the removal of dye per gram of adsorbent upsurges through growing adsorbent measure from 0.02 to 0.1 g. At developed quantity of adsorbent, commanded to amplify external expanse and extra adsorption places are obtainable producing advanced exclusion of the colorant. Additional intensification in adsorbent dosage did not origin any noteworthy intensification in % exclusion of colorant. This was outstanding to the load of colorants touched at equipoise rank midst solution and solid segment.

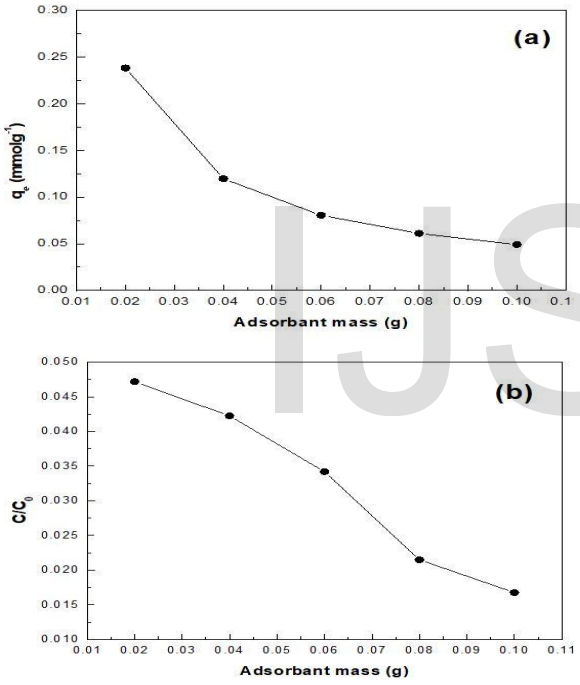

Fig. 4. Effect of sorbent dose on adsorption using: (a) sorption capacity *vs*. sorbent dose, (b) relative residual concentration (C/C_0) *vs*. sorbent dose (C_0: $2x10^{-4}$ M; T: 25 °C; pH 11).

3.5. Kinetics studies

The amount of deletion of verified colorant through adsorption was speedy primarily and formerly decelerated progressively till it reached equipoise elsewhere which here was noteworthy upsurge trendy percentage of exclusion. Extreme adsorption remained pragmatic at 60 min. and that one is therefore immobile as the steadiness period. Pointing at assessing the kinetics of adsorption is confirmed colorant against CC/MWCNTs, the pseudo-second-order and pseudo-first-order kinetic replicas were castoff to acceptable the investigational information, rendering to the underneath kinetic classical equations (Table 1).

The Lagergren of pseudo first order rate limite [23] is illustrated by Eq. (4):

$$\log (q_e - q_t) = \log q_e - k_1 t \quad (4)$$

The kinetic model of pseudo second order [24] is illustrated by Eq. (5):

$$t/q_t = 1/k_2 q_2^2 + 1/q_2 t \quad (5)$$

wherever qt is the quantity of colorant adsorbed (mmol/g) at several periods t, and qe is the supreme adsorption measurements (mmol/g) for Lagergren adsorption; and k_1 is the constant pseudo-first-order degree for the adsorption procedure (min^{-1}); q_2 is the supreme adsorption volume ($mmol.g^{-1}$) for the pseudo-second-order adsorption; k_2 is the pseudo-second-order adsorption rate constant ($gmol^{-1}min^{-1}$). Straight-line conspiracies of log ($q_e - q_t$) *vs*. t for the reaction of pseudo-first-order and t/q_t *vs*. t for the reaction of pseudo-second-order (see Figs. 5 and 6) for the adsorption of confirmed colorant against (CC/MWCNTs) have similarly been confirmed to attain the degree limits. The k_2, k_1, q_2, q_e, and connection coefficients, r_2^2 and r^2 for the dye underneath dissimilar temperatures remained considered since these conspiracies and stand specified in Table 2.

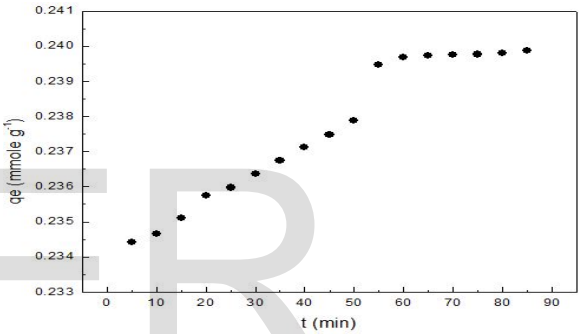

Fig. 5. Uptake kinetics using adsorbent: (pH 11; T: 25 °C; C_0: $2x10^{-4}$ M).

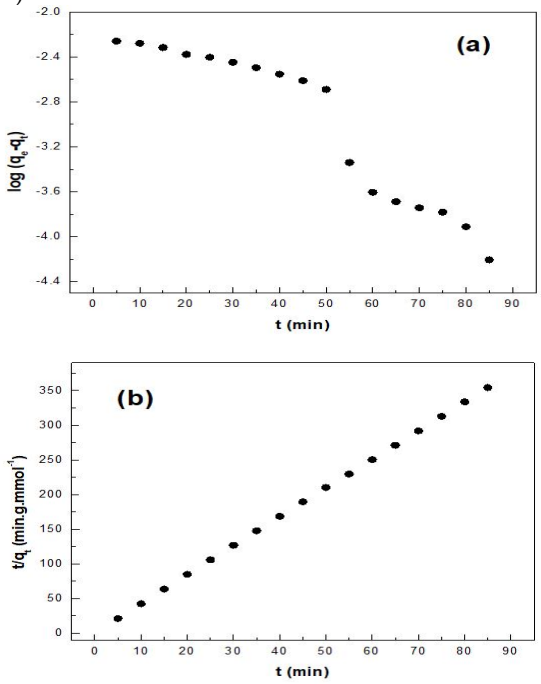

Fig. 6. Modeling of uptake kinetics with: (a) pseudo first order rate expression, (b) pseudo second order rate expression.

Meanwhile neither the pseudo-second-order nor the pseudo-first-order model can recognize the dispersion mode of action; the kinetic consequences were additional examined for dissemination mode of action by applying the model of intra particle diffusion. The consequence of intra particle dispersion persistent (interior superficial and opening dispersion) on adsorption container be strongminded through the subsequent calculation [25] (Table 1).

$q_t = k_{id}t^{1/2} + I$ (6)

wherever the intercept is I and k_{id} the intra particle diffusion rate constant ($mg.g^{-1}.h^{-1/2}$) which is strongminded from the linearity plot of q_t *vs.* $t^{0.5}$ (Fig. 7), and can be used to equate mass transmission loupes. Affording to this classical, the conspiracy of removal, q_t, *vs*. square root of time, $t^{1/2}$ must be linear if intra particle dispersion is intricate in the adsorption procedure and if these lines pass over the origin, and diffusion of intra particle is the rate supervisory stage.

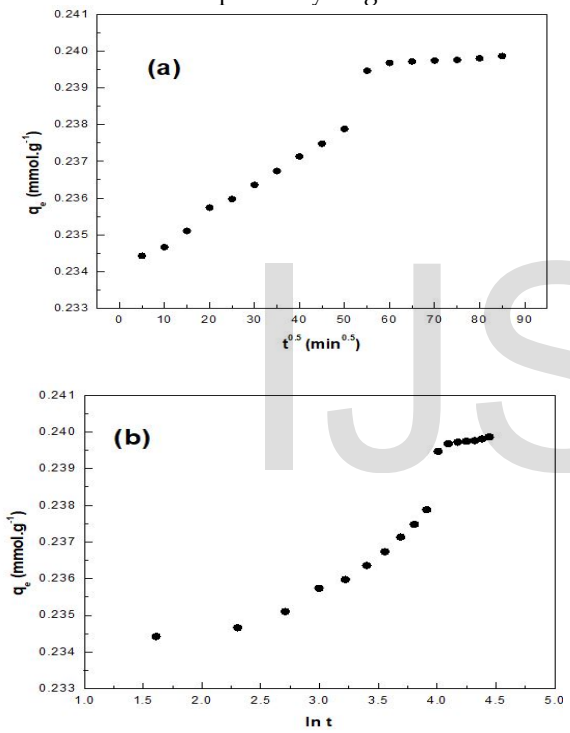

Fig. 7. Modeling of uptake kinetics with (a) simplified model of resistance to intraparticle diffusion (Morris and Weber equation), and (b) Elovich equation.

The rate constant of intra particle diffusion and the intercept principles are exhibited in Table 2. The Elovich comparation (Table 1) is castoff for universal claim to chemical adsorption [26]. The identical calculation is repeatedly legal for organizations in which the adsorbing external is not homogeneous, and is verbalized using Eq. 7:

$q_t = (1/\beta) \ln (\alpha\beta) + (1/\beta) \ln t$ (7)

wherever β is the relation of coefficient with the postponement of enclosed exterior and chemical adsorption of activation energy (g/mg) and α is the chemical adsorption rate (mg/mg min). Plot of q_t *vs*. ln t denote a linear connection with an intercept of (1/β) ln (αβ) and (1/β) slope. The value of 1/β imitates the quantity of locations obtainable conscience adsorption however the (1/β) ln (αβ) value designates the amount of adsorption when ln t equivalent go to zero point. Upon comparison among the kinetic models, the R^2 ideals of the classical pseudo-second-order kinetic (0.999) are considerably advanced more than individuals of classical pseudo-first-order kinetic (0.948), indicating the kinetics of CV adsorption follows the model of pseudo-second-order kinetic (Table 2). The rate-limiting phase in these adsorption procedures can be chemisorption connecting sturdy forces over the distribution or replacing of electrons amongst sorbate and sorbent [27]. The curve of intra particle dispersion gives multi linearity; and not pass by the origin. The kinetic model of intra particle diffusion (R^2 = 0.942) was measured from the slope of the second linear stage (Fig. 7). It is anticipated that in the original phases of adsorption (preliminary shrill growth) the exterior confrontation with mass transfer adjacent to the constituent part will be noticeably solitary. The additional lined serving is the steady adsorption phase through regulating intraparticle dispersion [28]. Elovich calculation undertakes the dynamic spots of the adsorbent are not homogeneous and consequently, display diverse activation energies of chemi-sorption. After growing the dye concentration, it was detected that the constant α (related to chemi-sorption rate) enlarged and the constant β (connected to the superficial exposure) reduced (Table 2), which is because of the reduction in the accessible adsorption exterior for the adsorbates. Consequently, by growing the concentration, in the interior the range calculated, the rate of chemi-sorption can be enlarged [29]. Hence, the kinetics of adsorption can be reasonably approached by the classical of pseudo-second-order kinetic, founded on the statement that the limiting step rate possibly will be chemi-sorption concerning electrostatic forces over the distribution and/or argument of the electrons amongst adsorbate and adsorbent [30,31].

TABLE 1. The linear forms of the kinetic models.

Kinetic model	Non-Linear form	Linear form	Plot	Ref.
Pseudo First order	$q_t = q_e[1-e^{-k_1 t}]$	$\log(q_e - q_t) = \log q_e - (\frac{k_1}{2.303})t$	$\log(q_e - q_t)$ *vs.* t	[23]
Pseudo Second order	$q_t = \frac{k_2 t}{1 + k_2 q_e t}$	$\frac{t}{q_t} = \frac{1}{k_2 q_e^2} + (\frac{1}{q_e})t$	(t/q_t) *vs.* t	[24]
Intra-particle diffusion	-	$q_t = k_i t^{0.5} + X$	q_t *vs.* $t^{0.5}$	[25]
Elovich equation	$\frac{dq_t}{dt} = \alpha e^{-\beta q}$	$q_t = \frac{1}{\beta}\ln \alpha\beta + \frac{1}{\beta}\ln t$	q_t *vs.* lnt	[26]

Table 2. Kinetic parameters for CV adsorption.

PFORE			PSORE			Weber and Morris model			Elovich equation		
k_1 (a)	$q_{e,calc}$ (b)	R^2	k_2 (c)	$q_{e,calc}$ (b)	R^2	Ki (d)	X	R^2	α (e)	β (f)	R^2
-0.03	0.26	0.891	9.629	0.24	0.999	$7.8x10^{-5}$	0.2	0.94	1.26	421.9	0.86

Units: (a): min^{-1}; (b): $mg.g^{-1}$; (c): $gmg^{-1}min^{-1}$; (d): $mg.g^{-1}$ min 0.5; (e): mg $g^{-1}min^{-1}$; (f): g mg^{-1}.

3.6. Adsorption isotherms

Numerous models of isotherm (Table 3) have remained castoff for seeing the steadiness adsorption of complexes from media like Langmuir [32,33], Dubinin Radushkevich [34] Freundlich [35], Dubinin Radushkevich [34] and Temkin [36]. Langmuir's classical isotherm adopts the undeviating adsorption energies onto the superficial adsorbent. It is created on supposition of the presence of monolayer adsorption on a wholly standardized superficial through a limited amount of indistinguishable positions and with insignificant collaboration amongst adsorbed fragments [32]. The Freundlich model is an empirical calculation created on adsorption of diverse external or surface supportive locations of diverse empathies [33]. The isotherm of Dubinin–Radushkevich originally for the subcritical fumes of adsorption on micro-pore objects subsequent a hole satisfying mechanism. This one is practical to differentiate the chemical and physical adsorption for eliminating a particle after its position in the sorption interplanetary to immensity [35]. The isotherm of Temkin shoulders of all particles in the phase reductions linearly once the coating is enclosed and the adsorption has a determined energy spreading of unchanging bond [36]. The forms of rectilinear and non-linear isotherm models of Langmuir, Dubinin–Radushkevich, Freundlich, and Temkin and their limitations are publicized in Table 4, wherever qe the quantity adsorbed of colorant at equipoise load (mmol/g), qm is the extreme sorption volume (consistent to the fullness of the monolayer, mmol/g), and Langmuir binding constant, K_L which is connected to the sorption energy of (L/mmol), C_e is the CV load at equilibrium in medium (M). The K_F (mmol/g) (L/mmol) 1/n and n are the constants of Freundlich connected to the sorption capacities and strength, correspondingly. KDR (J^2mol^{-2}) is the sorption energy constant, QDR (mmol/g) is the hypothetical fullness volume; ε is the Polanyi potential (J^2mol^{-2}). The gas constant R is (8.314 $Jmol^{-1}K^{-1}$), The temperature where the adsorption happens is T, K_T (L/mmol) is the constant of Temkin isotherm, The Temkin constant (βT, $J.mol^{-1}$) in relation to the heat adsorption. The isotherm model of Langmuir was originated as the greatest appropriate classical for recitation the adsorption isotherm of the CV dye into the CC/MWCNTs sorbent (Figs. 8 and 9). The lines of Freundlich diverged from the investigational number's arguments (Fig. 8). The model of Langmuir which obtainable the great association coefficient (R^2 = 0.995) can philanthropical a suggestion that chemisorptions (Demonstrated by kinetic revisions) [37]. The qm designed from the isotherm of Langmuir was nearby to the investigational qmax. Classical isotherm furnishings as marketed in Fig. 9.

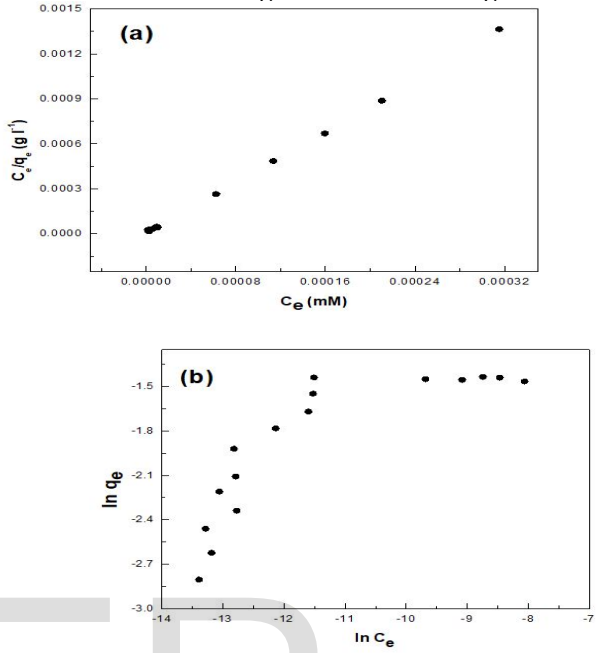

Fig. 8. Linearized plots for sorption isotherms: (a) Langmuir equation; (b) Freundlich equation.

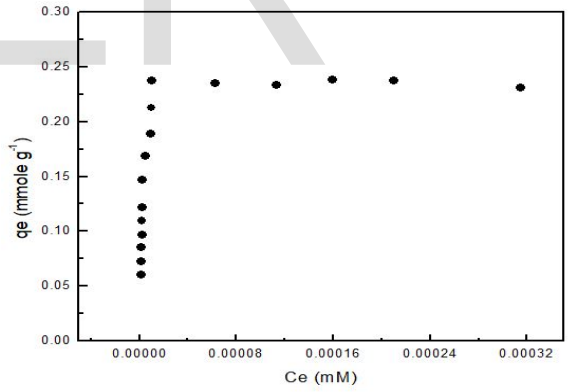

Fig. 9. Adsorption isotherms onto the adsorbent (Langmuir equation) (pH 11; T: 25 °C).

Examination of the isotherm constraints projected by Dubinin-Radushkevich was designed (Table 4). Isotherm stayed industrialized interested in explanation the consequence of spongy construction of sorbent and energy complicated in the procedure of sorption. The consequences of the isotherm of Dubinin Radushkevich are described in Fig. 10. The sorption's nasty energy value is 19.50 kJ/mol, indicating that a reaction to chemisorption. Certainly, it is normally acknowledged that 8 kJ/mol is the boundary energy for distinctive, physical (< 8 kJ/mol) and chemical sorption (> 8 kJ/mol). An assessment of the standard correlation coefficients gotten from the isotherm of Langmuir, Dubinin Radushkevich, Freundlich and Temkin representations (Table 4), discloses that the Langmuir correla-

tion coefficients are greater than the other models. The outcome proposes that the removal happens by monolayer sorption and homogenous. The position of the representations as survey: Langmuir > Dubinin-Radushkevich > Temkin > Freundlich.

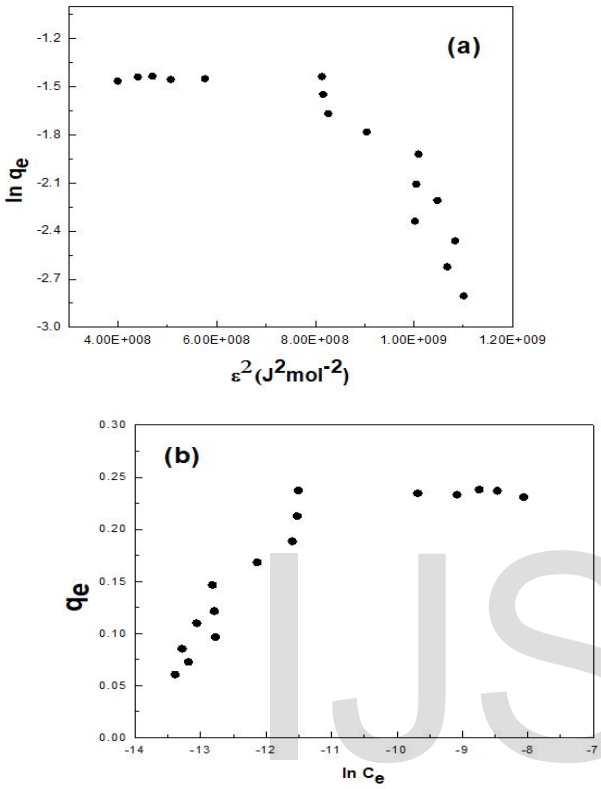

Fig. 10. Linearized plots for sorption isotherms: (a) Dubinin Radushkevich equation, (b) Temkin model.

Table 3. Sorption isotherms and their linear forms.

Isotherm	Non-Linear form	Linear form	Plot	Author
Langmuir	$q_e = \frac{q_{m,L} K_L C_e}{1 + K_L C_e}$	$\frac{C_e}{q_e} = \frac{C_e}{q_{m,L}} + \frac{1}{K_L q_{m,L}}$	$\frac{C_e}{q_e}$ *vs.* C_e	[33]
Freundlich	$q_e = K_F C_e^{1/n}$	$\ln q_e = \ln K_f + \frac{1}{n} \ln C_e$	$\ln q_e$ *vs.* $\ln C_e$	[35]
Dubinin–Radushkevich	$q_e = Q_{DR} e^{-K_{DR}\varepsilon^2}$	$\ln q_q = \ln Q_{DR} - K_{DR}\varepsilon^2$	$\ln q_e$ *vs.* ε^2	[34]
Temkin	$q_e = \frac{RT}{b_T}[\ln(A_T C_e)]$	$q_e = (\frac{RT}{b_T})\ln A_T + (\frac{RT}{b_T})\ln C_e$	q_e vs. $\ln C_e$	[36]

3.7. Thermodynamic parameters

Principles of thermodynamic limitations are the authentic pointers for real claim of a procedure. To achieve thermodynamic limitations for the adsorption structure, the quantity of adsorbed dye on (CC/MWCNTs) at equipoise and temperatures 20, 25, 30, 35, 40, 45 °C was scrutinized. The constant rate of the pseudo-second-order of CV dye adsorption is articulated as a meaning of temperature by Arrhenius relationship [38]:

$$\ln k_2 = \ln A - E_a/RT \quad (8)$$

Wherever A is the Arrhenius factor, R is the gas constant (8.314 J.mol^{-1}K^{-1}), Ea is Arrhenius activation energy and T is the functioned temperature. The linear adsorption plot of ln k_2 *vs*. 1/T was constructed to produce the triggering energy from the slope (–E_a/R) (Fig. 11).

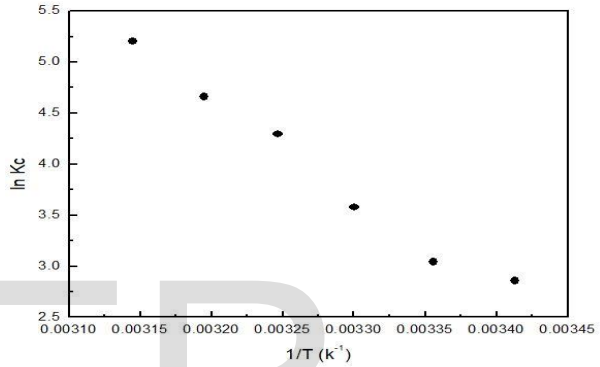

Fig. 11. Van't Hoff plots for adsorption onto the adsorbent.

The activation energy obtained is +13.25 kJ mol^{-1} for CV dye adsorption (CC/MWCNTs), which is representative of the low slung potential of the adsorption and consistent with chemisorption (Table 5) [39]. The additional thermodynamic limits, alteration in the typical enthalpy (ΔH^o), entropy (ΔS^o) and free energy (ΔG^o) were strongminded by means of subsequent calculations:

$$K_C = C_A/C_S \quad (9)$$

$$\Delta G^o = -RT \ln K_C \quad (10)$$

$$\text{Ln } K_C = \Delta S^o/R - \Delta H^o/RT \quad (11)$$

where C_A is the quantity of adsorbed dye on the (CC/MWCNTs) of CV solution at equipoise (mol/L), K_C is the equilibrium constant and C_S is the equipoise load of the dye in the medium (mol/L). The q_2 of the pseudo second order classical was castoff to gain C_S and C_A (Table 2). R is the gas constant and T is the temperature of the medium. From the plot of van't Hoff, ln K_C *vs*. 1/T (Fig. 11), the ΔH^o and ΔS^o were intended from the slope and the intercept, correspondingly. The principles thermodynamic of adsorption strictures are recorded in Table 5. The negative value of the free energy shift (ΔG^o) allows for the creation of adsorption and also defines the impulsiveness of the adsorption procedure [39]. The Negative value of the typical enthalpy revolution (ΔH^o) is (–76.44 kJ/mol) approving the exothermic nature of adsorption and proposes that the adsorption is chemical in nature connecting sturdy forces finished the distribution or swapping of electrons amongst sorbent and sorbate, thus representative that

the procedure is steady dynamically [40]. The positive assessment of standard entropy change (ΔS^o) which is (0.283 $J.mol^{-1}.K^{-1}$) proposes haphazardness at the solid/solution boundary through approximately mechanical variations in the adsorbent and the adsorbate [41,42].

Table 5. Standard enthalpy, entropy and free energy changes for adsorption.

3.8. Desorption studies

The cationic dyes desorption is commonly functioned by the alteration of pH. Generally, desorption is achieved in acidic circumstances. Renaissance of the inspected sorbent (CC/MWCNTs) was supported by insertion 0.02 g of CC/MWCNTs in the bottle and then washes away sensibly by sinuous purified water. Adsorbent overloaded by CV dye was then imperiled for renaissance by means of 0.1 M HCl. Subsequently renaissance the sorbent was once more prudently wash away with distilled water to develop complete for the additional track of removal [43,44]. The renaissance efficacy for individually adsorption/desorption sequence was originated to be 96.2, 94.5, 91.4%. This specifies that amalgamated has respectable presentation for recurring wear out to at tiniest 3 cycles [45,46]. The effectiveness of renaissance was considered by means of the subsequent calculation [7]. Sorption/desorption procedure was supported out for three sequences. Similarly, the developed effectiveness upon reprocess recommends recyclability and that acidic media is identically appropriate to the withdrawal of the CV from the disbursed adsorbent.

Table 4. Parameters of the sorption isotherm models.

Langmuir model				Freundlich model			Dubinin-Radushkevich (D-R) model				Temkin model		
$q_{m,exp}$ (a)	$q_{m,L}$ (a)	K_L (b)	R^2	n	K_F (c)	R^2	Q_{DR} (a)	K_{DR} (d)	Ea (kJ mol^{-1})	R^2	A_T (e)	b_T (f)	R^2
0.231	0.236	475201.91	0.999	4.921	0.429	0.645	-0.597	$-1.577x10^{-9}$	19.50	0.691	16.870	81311.85	0.732

Units: (a): mmol g^{-1}; (b): L $mmol^{-1}$; (c): mmol g^{-1} (L $mmol^{-1}$)$^{1/n}$; (d): J^2 mol^{-2}; (e): kJ mol^{-1}; (f): L mol^{-1}.

Table 5. Standard enthalpy, entropy and free energy changes for adsorption.

$-\Delta H^o$ (kJ mol^{-1})	ΔS^o (J mol^{-1} K^{-1})	T (K)	$-\Delta G^o$ (kJ mol^{-1})					
			293	298	303	308	313	318
76.44	0.283		159.41	160.83	162.25	163.66	165.08	166.49

4. Conclusions

In addition, the nanotubes of calcium carbonate/multiwalled carbonate (CC/MWCNTs) are functional adsorbent to remove CV dye from the aqueous media. Great adsorption measurements of CV dye on CC/MWCNTs in extremely alkaline media (pH=11) is outstanding to the durable electrostatic connections amongst its adsorption spot and dye cation. Further than 75 % exclusion effectiveness was gotten exclusively in 75 min. by adsorbent measure of 0.02 g aimed at preliminary CV load of 30-100 mg/L by pH 11. Brunauer Emmett Teller (BET) superficial expanse and Barrett Joyner Halenda (BJH) opening capacity were intended and originated to remain 55.134 m^2g^{-1} and 0.093 cm^3g^{-1}, correspondingly. SEM imageries display glowing definite and categorized morphological descriptions that are apparent for the operative adsorption of CV dye fragments on the hollows and holes of the (CC/MWCNTs). Designed for the claim of Freundlich and Langmuir calculations, the investigational consequences display that the model of Freundlich remained the superlative. The kinetic information has a tendency for fitting the model of pseudo second order kinetics with great correlation coefficients. Adsorption activation energy was similarly assessed and originated to be +19.50 $kJ.mol^{-1}$ representing chemisorption of the adsorption process. The ΔG^o principles stayed negative; consequently, the adsorption stayed impulsive in environment. Negative value of ΔH^o discloses that the progression of adsorption stayed exothermic. The ΔS^o positive value of suggests that the augmentation of a neatness amongst the adsorbate fragments and the adsorbent fragments. Growing the loads of sodium chloride scarcely distresses the sorption measurements. CV anions can be professionally desorbed from loaded CC/MWCNTs with acidic media and that sorbent can be reprocessed.

REFERENCES

[1] J. Bi, S. Zhao, J. Wu, Y. Xu, Z. Wang, Y. Han, X. Zhang, Appl. Organomet. Chem., (2020) e5552.
[2] A.A.P. Khan, A. Khan, M.M. Rahman, A.M. Asiri, M. Oves, Int. J. Biol. Macromol., 89 (2016) 198–205.
[3] N.G. Tsierkezos, S.H. Othman, U. Ritter, L. Hafermann, A. Knauer, J.M. Köhler, C. Downing, E.K. McCarthy, Sensors Actuators B Chem., 231 (2016) 218–229.
[4] W.-K. Li, H.-X. Zhang, Y.-P. Shi, Appl. Surf. Sci., 416 (2017) 672–680.
[5] R.A. Ahmed, A.M. Fekry, R.A. Farghali, Appl. Surf. Sci., 285 (2013) 309–316.
[6] A. Blanco-Flores, A. Colin-Cruz, E. Gutierrez-Segura, V. Sanchez-Mendieta, D.A. Solis-Casados, M.A. Garrudo-Guirado, R. Batista-Gonzalez, Environ. Technol., 35 (2014) 1508–1519.
[7] N. Hassan, A. Shahat, A. El-Didamony, M.G. El-Desouky, A.A. El-Bindary, J. Mol. Struct., 1210 (2020) 128029.
[8] A. Srinivasan, T. Viraraghavan, J. Environ. Manag., 91 (2010) 1915–1929.
[9] A. Mohamed, R. El-Sayed, T.A. Osman, M.S. Toprak, M. Muhammed, A. Uheida, Environ. Res., 145 (2016) 18–25.
[10] K.Z. Elwakeel, A.A. El-Bindary, A. Ismail, A.M. Morshidy, J. Dispers. Sci. Technol., 38 (2017) 943–952.
[11] K.Z. Elwakeel, A.A. El-Bindary, E.Y. Kouta, E. Guibal, Chem. Eng. J., 332 (2018) 727–736.
[12] A.A. El-Bindary, H.A. Kiwaan, A.F. Shoair, A.R. Hawas, Desalin. Water Treatment, 151 (2019) 145–160.
[13] M. Avila, T. Burks, F. Akhtar, M. Göthelid, P.C. Lansåker, M.S. Toprak, M. Muhammed, A. Uheida, Chem. Eng. J., 245 (2014) 201–209.
[14] S.B. Daffalla, H. Mukhtar, M.S. Shaharun, J. Appl. Sci., 10 (2010) 1060–1067.
[15] J.G. Yu, L.J. Zhang, B. Cheng and Y.R. Su, J. Phys. Chem. C, 111 (2007) 10582–10589.
[16] M. Rajabi, B. Mirza, K. Mahanpoor, M. Mirjalili, F. Najafi, O. Moradi, H. sadegh, R. Shahryari-ghoshekandi, M. Asif, I. Tyagi, S. Agarwal, V.K. Gupta, J. Ind. Eng. Chem., 34 (2016) 130–138.
[17] M.S. Derakhshan, O. Moradi, J. Ind. Eng. Chem., 20 (2014) 3186–3194.
[18] T. Zehra, N. Priyantha, L.B L. Lim, Environ. Earth Sci., 75 (2016) 357–371.
[19] V.T. Le, C.L. Ngo, Q.T. Le, T.T. Ngo, D.N. Nguyen, M.T. Vu, Adv. Nat. Sci.: Nanosci. Nanotechnol., 4 (2013) 035017.
[20] M.S. Dresselhaus, G. Dresselhaus, R. Saito, A. Jor M.S. Dresselhaus, A. Jorio, M. Hofmann, G. Dresselhaus, R. Saito, Nano Lett., 10 (2010) 751–758.
[21] J. Simmons, B. Nichols, S. Baker, M.S. Marcus, O. Castellini, C.S. Lee, R. Hamers, M. Eriksson, J. Phys. Chem. B, 110 (2006) 7113–7118.
[22] G.M.D. Ferreira, M.C. Hespanhol, J. de Paula Rezende, A.C. dos Santos Pires, L.V.A. Gurgel, L.H.M. da Silva, Colloids Surf. A, 529 (2017) 531–540.
[23] S. Lagergren, Handlingar, 24 (1898) 1–39.
[24] Y.S. Ho, G. McKay, Chem. Eng. J., 70 (1998) 115–124.
[25] W.J. Weber, J.C. Morris, Am. Soc. Civ. Eng., 89 (1963) 31–60.
[26] J. Zeldowitsch, Acta Physicochim. URSS, 1 (1934) 364–449.
[27] S.E. Subramani, D. Kumaresan, N. Thinakaran, Desalin. Water Treat., 57 (2016) 7322–7333.
[28] M.H. Dehghani, A. Dehghan, A. Najafpoor, J. Ind. Eng. Chem., 51 (2017) 185–195.
[29] Y. Zhang, G. Huang, C. An, X. Xin, X. Liu, M. Raman, Y. Yao, W. Wang, M. Doble, Sci. Total Environ., 595 (2017) 723–732.
[30] I.D. Mall, V.C. Srivastava, N.K. Agarwal, I.M. Mishra, Colloid. Surf. A, 264 (2005) 492–501.
[31] R.S. Juang, F.C. Wu, R.L. Tseng, Environ. Technol., 18 (1997) 525–531.
[32] I. Langmuir, J. Am. Chem. Soc., 39 (1917) 1848–1906.
[33] I. Langmuir, J. Am. Chem. Soc., 40 (1918) 1361–1403.
[34] M.M. Dubinin, E.D. Zaverina and L.V. Radushkevich, Zh. Fiz. Khim., 21 (1947) 1351–1362.
[35] H.M.F. Freundlich, W. Heller, J. Am. Chem. Soc., 61 (1939) 2228–2230.
[36] M.I. Temkin, V. Pyzhev, Acta Physicochim. URSS, 12 (1940) 217–222.
[37] A.R. Alley, Water Quality Control Handbook, McGraw-Hill Education, Europe, London, 2000.
[38] H. Nollet, M. Roels, P. Lutgen, P. Van der Meeren, W. Verstraete, Chemosphere, 53 (2003) 655–665.

[39] M.J. Jaycock, G.D. Parfitt, Chemistry of Interfaces, Ellis Horwood Ltd, Onichester, 1981.
[40] S.A. Chaudhry, T.A. Khan, I. Ali, J. Mol. Liq., 236 (2017) 320–330.
[41] C. Prasad, S. Karlapudi, P. Venkateswarlu, I. Bahadur, S. Kumar, J. Mol. Liq., 240 (2017) 322–328.
[42] N. Hassan, A. Shahat, A. El-Didamony, M.G. El-Desouky, A.A. El-Bindary, Mor. J. Chem., 8(3) (2020) 627–637.
[43] J. Liu, H. Yu, Q. Liang, Y. Liu, J. Shen, Q. Bai, J. Colloid. Interf. Sci., 497 (2017) 402–412.
[44] S. Li, M. He, Z. Li, D. Li, Z. Pan, J. Mol. Liq., 230 (2017) 520–528.
[45] E.N. Seyahmazegi, R. Mohammad-Rezaei, H. Razmi, Chem. Eng. Res. Design, 109 (2016) 824–834.
[46] Y. Wang, C. Pan, A. K. Vipin, L. Sun, W. Chu, Nanomater., 8 (2018) 1–26.